Section 7

DESIGN/TEST CRITICAL COMPONENTS

7.1 LOW PRESSURE DROP RECUPERATOR

This work constituted WBS 2.8.1 on the ATS program. Topical Report 8.1 should be consulted for more details of this work.

7.1.1 Introduction

Solar's Primary Surface Recuperator (PSR) technology is based on 24 years of development and operational experience. This technology has typically been applied to relatively low pressure drop cycles having modest exhaust gas temperatures. One objective of the ATS program is to develop engines of much higher thermal efficiency resulting in engines that fire hotter and have higher exhaust gas temperatures. Other goals included lower emission, reduced cost of power and improved RAMD. Recuperator life prediction, creep modeling and performance prediction become even more important factors in the design.

In prior applications of the PSR performance has been predicted using an in-house analytical model. The accuracy of predictions has been notably good at design point. However, with an engine like ATS where high efficiency is such a salient and vital feature, predictions must be of the utmost accuracy, especially over the broad operating range of the turbine. Validation of the empirical models with upgrading where necessary was regarded as essential.

In this work, performance data have been obtained for the candidate heat transfer surface. Furthermore, performance data were obtained on a scaled rig to provide the necessary data to validate and calibrate the analytical model. The pretest predictions of air-side and gas-side pressure drop were in very good agreement with the actual test results. The predicted effectiveness also agreed well with that actually determined by experiment.

7.1.2 Background on the PSR

Solar's PSR technology is grounded in over two decades of development work that began at Caterpillar in the 1960s. Solar has improved on it in a significant way since 1981 and will fine tune the design even further with the development of a recuperator for ATS.

The PSR is made of thin, typically 0.003-inch type 347 stainless steel folded into a corrugated pattern. This pattern, shown in Figure 20, maximizes the primary surface area that is in direct contact with exhaust gas on one side and compressor discharge air on the other. Pairs of these sheets are welded together around the perimeter to form air cells (Figure 21), the basic building block of the

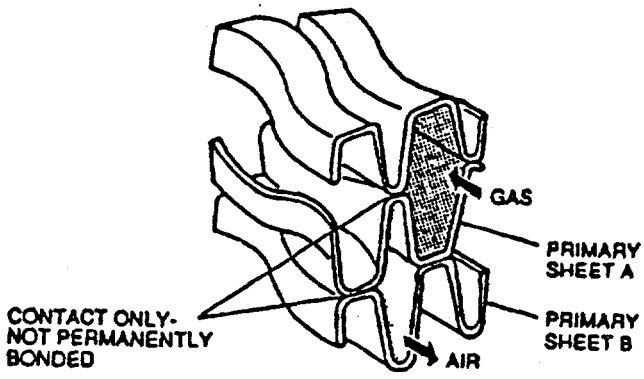

Figure 20. Primary Surface Sheets

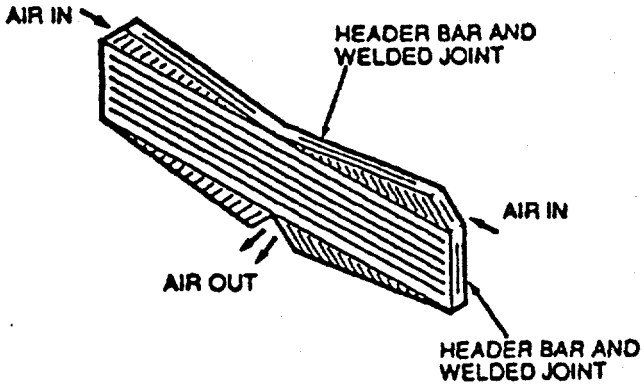

Figure 21. PSR Air Cell

PSR. Each cell is pressure checked before it is welded into the recuperator core assembly, as shown in Figure 22. There are no internal welds or joints within the air cell.

Once the completed recuperator core has been pressure checked, a thermally balanced restraint system (TBRS) is added to the core to contain the pressure forces. This is seen in Figure 23. The individual air cells consist of the thin folded sheets welded to header bars located at the air cell edge. The header bars are designed to resist internal pressure without support, but the primary sheets require full support to prevent "ballooning" under internal pressure.

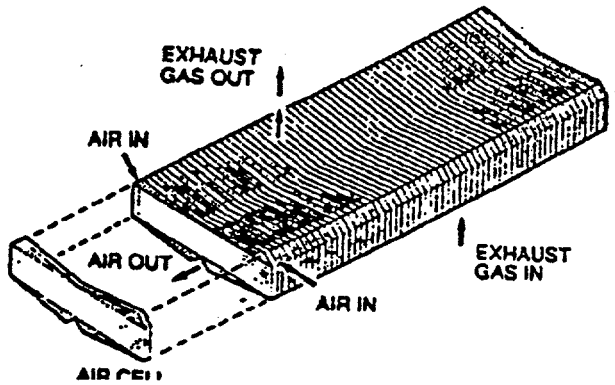

Figure 22. Core Assemblies

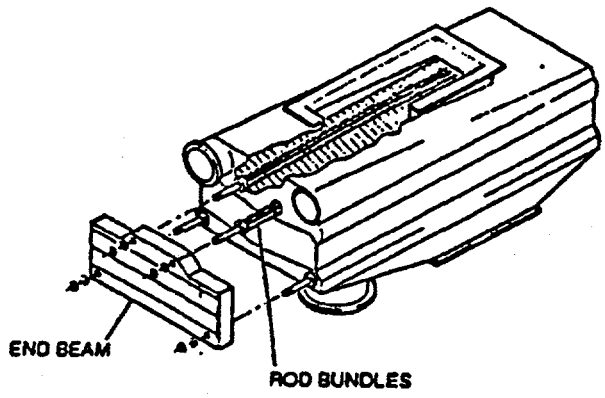

Figure 23. Thermally Balanced Restraint System

End beams are tied together by preloaded tie rods that are in the gas stream to assist in thermal transients.

The philosophy behind this design is explained more fully in Topical Report WBS 8.1 to which reference should be made for details.

Sheet metal ducting is added to the recuperator core, as required, to direct the air and exhaust gases through the recuperator assembly (Figure 24).

The recuperator assembly is mounted to the gas turbine in a manner essentially free of external loads due to piping reactions and thermal expansion. These features allow the recuperator to be easily and directly integrated with the turbine to obtain a very compact package.

7.1.3 Work Program

There were three major test series run in this program. These address heat transfer surface characterization, recuperator performance and life prediction. The latter is critical to satisfy customer's concerns but a goal of 100,000 hours of life means that this will remain an ongoing study rather than be completed and reported here.

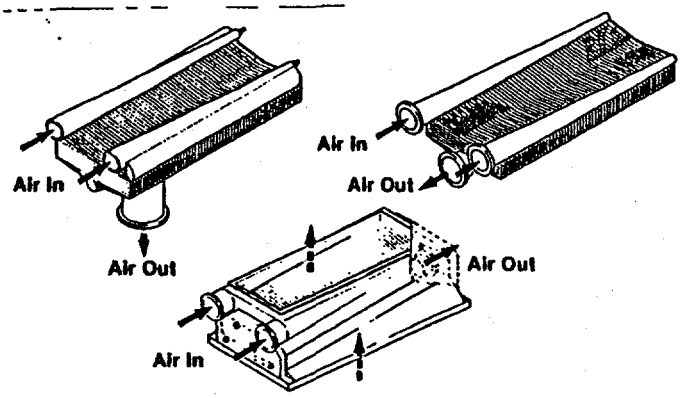

Figure 24. Air and Exhaust Gas Ducting

7.1.3.1 Life Prediction Work

Most recuperators fail as a result of a combination of thermal and pressure-induced mechanical cycling. Environmental influences, such as corrosion and oxidation, accelerate recuperator failure. The PSR is designed to substantially reduce all of these effects, be very reliable and require low maintenance.

The PSR design does not tie the structure with multiple interconnection points, but allows the individual components that make up an air cell and the air cells that makeup the overall recuperator core structure to absorb strain. These features give the PSR the ability to accommodate large thermal gradients under operating conditions. With the thermal stresses substantially reduced, the PSR structure can more easily handle the pressure forces.

Oxidation and corrosion resistance are important criteria to consider when selecting a material for PSR applications as the material's environmental resistance determines the long term durability of the recuperator. With the very thin materials used, a stable oxide film must be maintained to avoid excessive material loss.

For the majority of gas turbines operating at temperatures lower than 650°C (1200°F), type 347 stainless steel (18%Cr/10%Ni/1%Cb) provides excellent oxidation resistance. Its outstanding performance in this temperature range is derived from the presence of a thin, adherent Cr_2O_3 oxide film which forms in service at a predictable rate. This surface film inhibits further transport of oxygen to the underlying material, thus avoiding excessive oxidation damage.

Solar's experience in recuperator performance covers nearly two million hours total service with individual units approaching 50,000 hours. From this experience, it appears that oxidation governs the life of recuperators operating with low pressure ratio machines (in the absence of overtemperatures), and that creep of the cell under the high pressure compressor air may govern the life of units attached to medium pressure ratio gas turbines. The proper choice of materials can provide control of life limited by oxidation, although this must be done at an affordable cost. This work was delayed until the Phase III activity.

A flattened tube test was designed to determine dimensional changes of the PSR heat transfer surface profile after exposure. These data are to be used in the finite element creep modeling that is underway. The test was still in progress at the time this report was written. Data will be reported separately upon conclusion of the test. The flattened tube test was designed to provide strain data that are needed to characterize the deformation of the recuperator's primary surface folded fin under a high temperature and pressurized environment. The results of this study are intended to validate a finite element model used for static and creep analysis of the primary surface. The dimensions of the flattened tube, which is geometrically similar to the primary surface, are measured periodically to determine the deformation of the profile as a function of time.

Two thermocouples were attached on the test specimen to monitor temperatures during the test. High temperature strain gages were employed to measure the strain rate of the tubes. The tube samples were secured to a test specimen, basically held in place within a furnace by two plates bolted together, one on each end of the tube.

The Flattened Tube Test of type 347 stainless steel has been running since late 1994. The high temperature strain gages have saturated so are no longer providing data. However, dimensional changes have been monitored every two weeks. From all indications, these data will be invaluable in validating finite element modeling of the primary heat transfer surface. This work will be continued in Phase III.

7.1.3.2 Performance Predictions

A new high capacity air cell is to be used on the ATS recuperator. Heat transfer surface performance data are needed to support design of the recuperator and prediction of performance. The performance data for the old style air cell were used to size the recuperator. However, more representative heat transfer surface data are essential when it comes to accurate performance predictions.

Solar utilizes a variety of tools in designing a recuperator. One of the analytical tools developed in-house over the years is the two-dimensional (2D) analytical model which provides a basis for the aerothermal design, analysis, and prediction of performance of the primary surface recuperator. This analytical method is an integrated finite element heat transfer and fluid flow model for the corrugated counterflow core as well as the inlet and outlet oblique cross flow triangular headers. The method enables one to establish the flow distribution across the core and triangular headers and quantify the flow, temperature, static pressure, and mass velocity fields in the core, triangular headers, and the transition region between the two. The method was validated using limited empirical data on the old style primary surface recuperators.

A design called the High Capacity Air Cell module was used to measure performance. This module is 18.6 x 32.5 x 12.6 inches in dimensions and contains 100 air cells. Topical Report 8.1 gives full data on this test core. Conditions approximating the ATS at 100%, 70% and 30% power level were fed into this core. Thermal effectiveness, air-side pressure drop, and gas-side pressure drop were measured for these three power levels.

The approximate conditions of temperatures, pressures and flow rates had been based on the anticipated ATS design. When the cycle and operating conditions had been established more precisely, complete performance data were obtained in which planning of the work was aided by the approximate data.

Under the approximate operating conditions, the rig tests demonstrated design point performance goals, but lower than predicted effectiveness at part load mass flow rates. The heat balance deviation also exceeded the target value of 3%. It was anticipated that eliminating the leakage and mixing out the high gas-out temperature gradients would improve the energy balance deviation.

The high heat balance deviation problem encountered during these prior tests was substantially reduced by eliminating the rig leaks, adding a gas-out mixer and more insulation to minimize the heat losses from the rig. The energy balance deviation was brought below the 3% limit for the majority of the test points. At the lower mass flow rates the higher heat balance deviation was attributed to an internal core leak which may explain the large-than-normal deviation between predicted and measured effectiveness values. While the leaks were reduced for the majority of the test, they did increase as testing continued. The leaks that developed with this core were the result of a duct/core interface design that is not seen in a production core.

When testing was suspended, the recuperator core was removed from the rig for inspection and leak checking after a series of test data looked suspect. At pressures of 120 psia and mass flow rates

less than 3.14 lb/s the effectiveness dropped significantly, rather than remain relatively flat or increasing as seen in all other data trends from previous tests. To further investigate the problem, data was repeated at 56 psia inlet air pressure. The measured effectiveness was lower. The effectiveness diverged from the previous test results at lower mass flow rates.

A leak check confirmed a leak of about 1.8% of rated flow rate. Physical examination at the recuperator manufacturing facility showed five leaking air cells at the gas-in edges. These leaks had existed before the current test series started but had grown. The cell could be blocked but up to eight cells would have been non-functional. This was deemed too high so the testing on this core was suspended.

In spite of these problems, the performance goals were met at the rated conditions. The thermal effectiveness was measured at 90.3% and the total pressure drop was 6.8% with a energy balance deviation of 1.4%. Effectiveness values were somewhat lower than predicted values under part-load conditions. This effect has been observed in previous tests and may be due to some flow maldistribution, though this is speculation only. The measured data will be used to calibrate the 2D analytical model using the final results from the heat transfer surface performance test.

Test data are presented in extensive tables in Topical Report 8.1 and should be examined for details. Reasonably good agreement between the 2-D prediction and experimental effectiveness was obtained as illustrated in Figure 25.

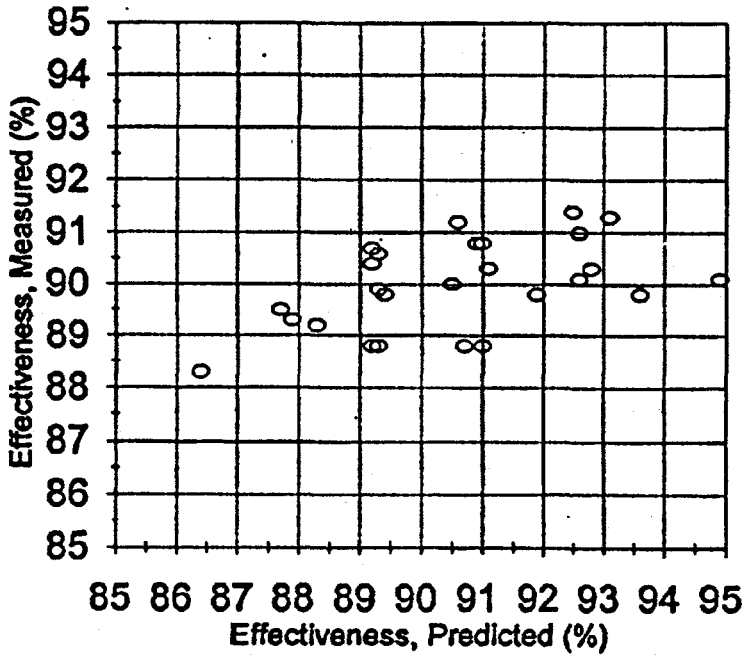

Figure 25. Comparison Between Predicted and Measured Thermal Effectiveness

7.1.3.3 Transient Tests

The transient test rig, shown in Figure 26, is used to measure the performance characteristics of heat transfer surfaces based on a transient single blow test technique developed at Stanford University. Pressure and temperatures of the air entering and exiting the rig are measured over a broad range of Reynolds numbers and are then correlated and used as a basis for establishing the

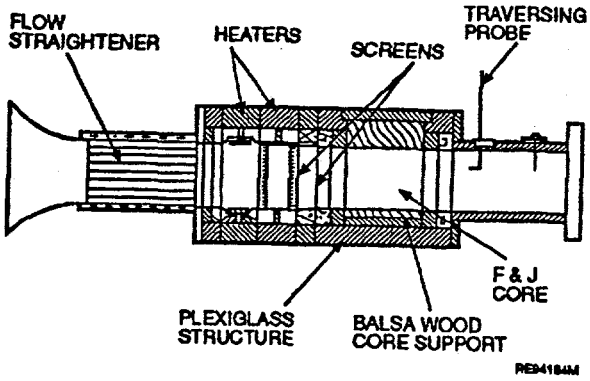

Figure 26. Transient Test Rig

convective conductance on the air- and gas-sides of the recuperator. These are the friction factor and Colburn modules data ("f" and "j" factors).

Details of the test rig and methods are available in Topical Report No. 8.1 and should be consulted for details.

7.2 SUBSCALE CATALYTIC COMBUSTOR

This work constituted WBS 2.8.2 on the ATS program. Topical Report 8.2 should be consulted for more details of this work.

7.2.1 Introduction

The catalytic combustor has been identified as a critical technical element in the commercialization of ATS. It has influence on both marketing and design. On marketing, it will provide market access to Air Quality districts from which gas turbines are now excluded. On design, it will produce a lower pattern factor than can now be achieved so that the boundaries of the gas flow passage in the turbine will experience higher temperatures but the peak temperature will be lower.

The Solar/DOE ATS engine program will reduce engine pollutant emissions to single digit levels and low pattern factor. Program goals include the attainment of emissions (NOx, CO and UHC corrected to 15% O_2) below 10 ppmvd over the 50 to 100% load range, pattern factor less than 0.2, and long term combustor component durability.

Catalytic combustion technology development in Phase II consisted of two main tasks: Task 2.8.2 involving the evaluation and demonstration of catalytic combustion technology in a subscale rig environment, and Task 2.8.5 involving the design and evaluation of a single can full-scale catalytic combustion system based on subscale results. Successful full scale rig operation will be followed by sector rig testing, and the procurement of a full set of engine hardware for an engine demonstration as part of Solar ATS Phase III program.

7.2.2 Background

Topical Report 8.2 discusses the three mechanisms by which oxides of nitrogen (NOx) are formed by combustion processes. It points out, further, that catalytic combustion extends the range of stable combustion to leaner fuel-air mixtures and lower temperatures than are possible with technologies such as Solar's industrially-accepted SoLoNOx combustor. The catalytic combustion process allows the adiabatic combustion temperature to be reduced below 2500°F. Topical report 8.2 should be consulted for more details.

Catalyst substrate materials capable of withstanding surface temperatures close to adiabatic combustion temperatures (typically 2400 to 2500°F) over long periods of catalyst operation are currently not available. The development of ceramics technology may provide substrates capable of sustaining extended periods of high temperature operation. However, the ability of ceramic substrates to withstand high thermal and mechanical shocks during engine startup and acceleration transients has not been demonstrated. The issue of long term durability of catalyst substrates and high catalyst activity for continuous operation for 8000 to 10000 hours has not been resolved. It is

unlikely that questions about durability of catalysts will be satisfactorily answered before a catalytic combustor is tested in the field. Alternate catalyst designs that limit substrate temperatures well below adiabatic combustion temperatures have recently become available.

7.2.3 Approach

The primary goal of Task 2.8.2 was to evaluate subscale catalysts beds (approximately 4 in. diameter) at inlet temperatures and pressures representative of the ATS-S engine cycle for reactor ignition and catalyst activity, emissions, fuel-air turn-down capability, and sensitivity to combustor operating variables. Subscale catalyst beds designed and supplied by Engelhard Corporation were tested in a high pressure test rig. As part of long term catalytic combustion system development, Solar entered into a technical collaboration with Catalytica Inc. to evaluate an alternate catalytic combustion technology for Solar ATS engines. Initial subscale work with Catalytica was performed under a Solar-funded program. This work had been focussed on the Solar Mars engine cycle, but was redirected to the ATS-S engine.

Solar's strategy for implementing catalytic combustion in an engine must consider both materials and system design issues. For example, since catalysts with a wide range of ignition temperatures are not available, incorporation of preburners may be required to increase gas inlet temperatures at some engine operating conditions. Investigation of catalyst designs that limit substrate temperatures well below the adiabatic combustion temperature may help resolve the durability issue. While ultra-lean catalytic combustion is an effective NOx inhibitor, it also limits the amount of air available for cooling combustor components. Thus, the performance of the catalyst as a component of the combustion system has important implications on overall system design. The sub-scale catalytic combustion program seeks to improve Solar's technical knowledge base about catalyst design, performance, and limitations. This information is critical to overall catalytic combustion system design to meet the challenges of engine start-up and acceleration, catalyst operation over a wide range of engine loads with low emissions, and long term component life and durability.

7.2.4 Catalyst Design Considerations

As mentioned earlier, Solar has teamed with Engelhard Corporation and Catalytica Inc. for the design and fabrication of catalyst beds. The catalyst designs used by both Engelhard and Catalytica depend on partial conversion of the fuel in the catalyst and completion of heat release through homogeneous gas-phase reactions downstream of the catalyst. The Engelhard catalytic reactor is a multiple piece bed design using a ceramic honeycomb substrate coated with catalytically active noble metals (e.g., Pd). The active catalyst material is proprietary. The Catalytica design uses a metal substrate and a Pd based catalyst. Figure 27 shows a schematic of the Catalytica combustion system, where catalyst substrate temperatures are kept low. Details of catalyst design are provided in Topical Report 8.2.

A catalyst has an operating window defined by three parameters: inlet gas temperature, adiabatic combustion temperature, and maximum allowable surface temperataure (see Figure 28). A certain minimum temperature is needed for catalyst ignition. Each stage of the catalyst has a maximum operating temperature to avoid degradation and to ensure long term durability.

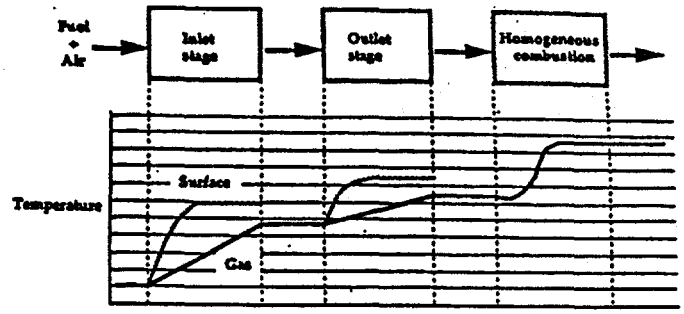

Figure 27. Schematic of Catalytica Catalytic Combustion System

Two sources of departure from the operating window are: inadequate combustor inlet gas temperature; and significant departures from the desired overall fuel-air (F/A) ratio. A typical catalyst ignition temperature is 700°F and is relatively independent of the fuel-air ratio. At ATS-S conditions a pre-burner is not required for catalyst ignition at part loads (up to 50% load).

Local departure from the overall fuel-air ratio is a major limitation for catalyst operation. Such departures may occur at part-load operation, as illustrated in Figure 28. The presence of pockets of fuel-air mixtures leaner than the overall fuel-air ratio could lead to higher CO emissions (for the same residence time), while rich pockets could cause catalyst damage due to local overheating. It is pointed out in the Topical Report that changes in the adiabatic flame temperature will affect the required residence time for rapid CO reduction to attain the goal of <10 ppmv.

The operation of the catalytic reactor requires a fuel preparation system capable of achieving nearly complete fuel-air premixing, while keeping the residence time in the premixer short to prevent autoignition, and avoiding regions of separated flow to prevent flashback. Operation of the catalyst bed over a wide load range (50 to 100%) requires variable geometry design. Moreover, even with the incorporation of variable geometry and high levels of fuel-air premixing, operation of the catalytic combustion system will require improved control over combustor operational variables to avoid high CO emissions or catalyst damage due to overheating of the catalyst substrate.

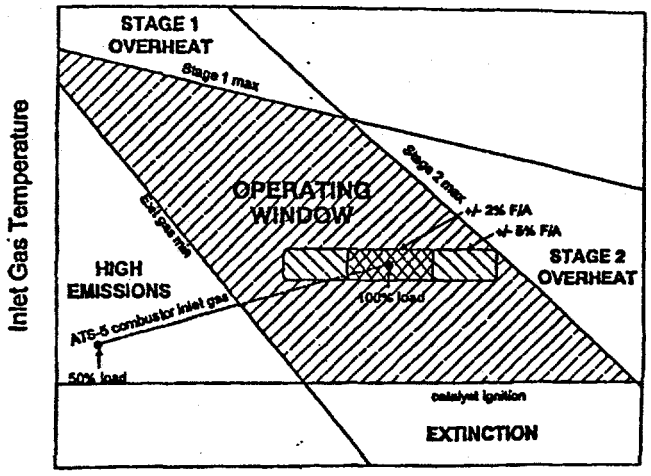

Figure 28. Typical Operating Window for Catalyst Bed

7.2.5 Subscale Rig Design Iterations

A subscale catalytic combustor test rig was used to evaluate different catalyst bed designs at various inlet temperatures and pressures. A schematic of the rig used during the early tests is shown in Figure 29. The rig consists of four stages: a preheat combustor; fuel-air premixer; catalyst bed; and a post catalyst combustor. The catalyst bed is enclosed in a catalyst can which can accommodate a bed 5 inches in diameters with a 4-inch diameter flow path. The preheat combustor incorporates a lean-premixed fuel injector, and is used to provide the required catalyst inlet temperature. The preburner is uncoupled from the catalytic premixer, and is located in the air supply pipe more than 15 diameters upstream of the premixer inlet.

The combustor test rig brings the pre-heated combustion air in a reverse flow configuration outside the combustor liner before entering the combustion chamber. This simulates the air flow path in the canted ATS multi-can gas turbine configuration.

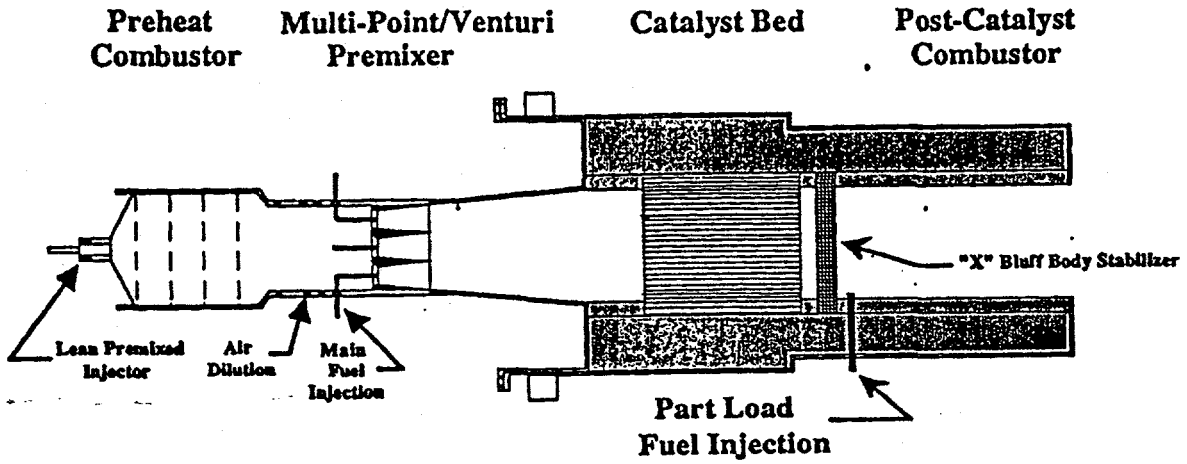

Figure 29. Basic Catalytic Combustor Test Rig

The operating window shown in Figure 28 is dependent to a very major extent on the uniformity and constancy of the fuel-air mixture. Several changes in premixer design, requiring considerable time and effort, were necessary to improve the fuel-air premixing at the inlet to the catalyst bed. These are described in detail in the Topical Report. Some of the premixing concepts that were evaluated included:

1. Constant diameter duct with multi-point fuel injection through tubes.
2. Constant diameter duct with multi-point fuel injection from the wall.
3. Multi-venturi with multi-point fuel injection.
4. Multi-point fuel injection in conjunction with static mixers.
5. Reverse flow premixer with multi-point fuel injection.

The premixer performance is critical to the success of the catalytic combustion system. Design objectives were to provide a fuel concentration variation of ±5%, a maximum temperature variation of ±14°C (±25°F), and a ±5% peak-to-mean variation in the velocity profile. The premixer performance was characterized initially through hydrocarbon concentrations measured at seven points upstream of the bed, and, later, through measurements using 33 sampling probes mounted on an inactive (uncoated) catalyst module. Some of the premixer designs were evaluated for regions of flow separation by constructing Plexiglas models, and performing flow visualization tests using a smoke generator.

7.2.6 Sub-Scale Test Results

A typical test of the subscale catalytic combustor includes rig and emissions equipment warm-up, preheat combustor ignition, part load combustor light-off, and combustor performance testing. Once air is preheated to the desired operating temperature, the preheat and part load combustors are ignited with torches. After stable flames are achieved, the torch is extinguished. At this point, main fuel is started to the catalyst bed and part load fuel is reduced to maintain a constant combustor

outlet temperature and pressure loss. Once the catalyst is fully ignited, part load fuel is stopped. Operational variables are then adjusted to the required conditions.

Once at the desired test pont, the burner is allowed to reach a thermally stable operating condition before data are recorded. Typically, at least ten minutes are allowed for the system to reach thermal equilibrium. During this stabilization period, the catalyst exit plane is visually inspected and exhaust emissions levels are monitored. When stable operation is achieved, test data are recorded using an automated data acquisition system.

Early work with Engelhard supplied catalyst beds concentrated on improving reactor light-off characteristics and activity, and optimization of catalyst bed length. Most of these tests were conducted using the multi-venturi premixer configuration. Based on seven point measurements, a peak-to-peak fuel concentration variation of 6.7% was determined. An optimum catalyst bed length of 10.5 inches was established based on test results. Testing under this configuration showed NOx emissions consistently below 3 ppmv (corrected to 15% O_2), but CO and UHC emissions as high as 1000 ppmv of CO and 250 ppmv of UHC (@ 15% O_2). Thermocouples in the bed showed a large difference in temperature between the center and the wall of the catalyst. Post-test inspection revealed damage to the catalyst due to the development of a hot spot (bed temperature >2500°F). These unsatisfactory test results led to a detailed characterization of the premixing with the multi-venturi design, using the 33 sampling probe configuration described in the Topical Report. Measurements indicated a 40% peak-to-peak variation in fuel concentration, and showed that the 7-point measurements greatly underestimated the inhomogeneities in fuel concentration.

A set of five static mixers was used to establish a baseline premixing level, and a Catalytica two-stage catalyst bed designed for the Solar Mars engine cycle was tested under this configuration. At full load Mars engine conditions, the test was conducted without a preburner, so that the contribution of the catalyst to NOx emissions could be determined directly. The catalyst used a 4-inch diameter cylindrical unit with a small center plug used for catalyst fabrication. The catalyst module ignited almost immediately and very uniformly. One hour of continuous steady state operation was maintained. Typical emissions in the range CO < 1.3 ppmv, UHC ~ 0.0 ppmv, NOx < 0.4 ppmv (corrected to 15% O_2) were recorded.

The fuel flow was then varied to study the effect of fuel turndown on catalyst operation. At a fuel/air ratio of 0.0355, CO emissions increased beyond 10 ppmv (@ 15% O_2). With the fuel flow close to full load conditions, the inlet gas temperature was decreased in steps to find the minimum operating temperature to maintain catalyst ignition. At an inlet gas temperature of 675°F, the catalyst remained uniformly ignited, and emissions were maintained under 2 ppmv (@ 15% O_2). Multiple light-off tests were conducted under Mars full load conditions. Every time the fuel was turned back on, the catalyst ignited, and the system returned to low emissions operation with no apparent change in performance.

Based on the satisfactory performance of the catalyst bed at Mars design conditions, a preliminary design of a Catalytica bed for ATS-S operating conditions was tested. Ultra-low emissions (<10 ppmv @ 15 O_2) of NOx, CO and UHC were obtained for short periods of catalyst operation. Further optimization of this catalyst design is needed to reduce the activity of stage 2, so that operation at fuel-air ratios corresponding to higher adiabatic temperatures is possible. This will enable the attainment of steady levels of low CO emissions. Post test inspection revealed the catalyst to be in good condition, and the catalyst was used in a later test.

As part of Solar's efforts to investigate alternate premixer designs, a reverse flow mixing device was evaluated among other options. Fuel is injected at multiple points using fuel tubes with multiple

orifices. Mixing measurements conducted at rig pressure and temperature were within the specification for the catalyst bed (maximum peak to peak variation <7%). A catalyst bed was sucessfully tested with this premixer (with ultra-low emissions) at ATS-S full load conditions.

7.2.7 Coordination With ATS Phase III

The technical basis to use catalytic combustion under ATS conditions was demonstrated with NOx consistently less than 3 ppmv and CO and UHC less than 10 ppmv.

7.3 AUTOTHERMAL FUEL REFORMATION

This work constituted WBS 2.8.3 on the ATS, Phase II program. Topical Report 8.3 gives an extensive discussion of this technology and should be consulted for more details.

7.3.1 Introduction

It was not planned to introduce this technology into the first generation of ATS, but the technology was regarded as critical for future generations of these turbines. For example, application of ATS to high speed marine transport (see Market Survey , WBS 2.5) requires use of a liquid fuel such as diesel. The ATR will make this possible, and, at the same time, will provide low emissions.

Autothermal fuel reforming (ATR) consists of reacting a hydrocarbon fuel such as natural gas or diesel with steam to produce a hydrogen-rich "reformed" fuel. There are several advantages to this processing of the fuel. The hydrogen-rich gas has a high flammability with a wide range of combustion stability. Being lighter and more reactive than methane, the hydrogen-rich gas mixes readily with air and can be burned at low fuel/air ratios producing inherently low emissions. The hydrogen-rich reformed fuel also has a low ignition temperature which makes low temperature catalytic combustion possible – another factor contributing to low NOx emissions. Also, ATR can be designed for use with a variety of alternative fuels including heavy crudes, biomass and coal-derived fuels. When the steam required for fuel reforming is raised by using energy from the gas turbine exhaust, cycle efficiency may be improved. The stack temperature is lower giving an additional advantage.

7.3.2 Background to Fuel Reformation Technology

Fuel reformation rearranges and reforms a primary fuel such as natural gas or diesel with steam, to produce a hydrogen-rich gaseous secondary fuel. The reformed fuel has a heating value (on a mass flow basis) greater than that of the parent fuel. The secondary fuels reformed from paraffinic materials have high hydrogen contents and this makes them desirable from an ease of combustion viewpoint. The wide range of combustion stability provided by the high hydrogen reformed fuel would also allow the operation of most combustion systems at low fuel/air ratios where low NOx is produced. Solid fuels such as coal, biomass, or other carbonaceous materials can also be reformed via gasification.

The fuel reformation with steam may formally be depicted by the following equations:

$$C_nH_m + n\,H_2O = n\,CO + (n + m/2)\,H_2 \quad [1]$$

$$CO + H_2O = CO_2 + H_2 \quad [2]$$

$$CO + 3\,H_2 = CH_4 + H_2O \quad [3]$$

When hydrocarbons (C_nH_m) in the fuel and steam (H_2O) are heated together to a temperature of approximately 1250 - 1500°F, the hydrocarbons begin to decompose and react with the steam to form hydrogen (H_2) and CO. Equation [1] is endothermic and is generally considered to be irreversible. The product distribution of steam reforming is governed by the water-gas shift [2] and methanation [3] reactions. In the fuel reforming, the rate-determining step appears to be the catalytic surface reactions between adsorbed CHx and OH species. It is generally agreed that the fuel reforming activity will be dependent on the accessibility of catalyst surface area where the surface being covered with adsorbed OH groups for reactions with the hydrocarbon fragments.

Steam reforming requires an external thermal input to cause reaction. In autothermal reforming, this energy is internally supplied by partial oxidation of a portion of the parent fuel,

$$C_nH_m + n/2\,(O_2 + 3.76\,N_2) = m/2\,H_2 + n\,CO + 1.88n\,N_2 \qquad [4]$$

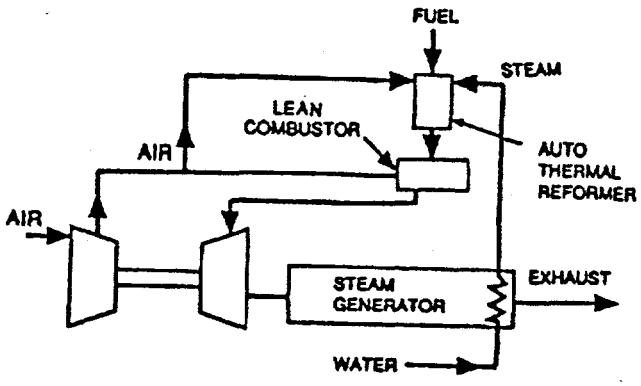

Figure 30. Integrated Steam/Fuel Reformer

In autothermal reforming, air ($O_2 + 3.76\,N_2$) reacts with parts of the fuel to provide heat. Then, when the bulk of fuel is heated by absorbing thermal energy, it dissociates into smaller fragments. The partial combustion reaction [4] is exothermic providing the energy for the intra-bed steam reforming reaction [1]. In practice a small quantity of fuel and air is burned separately and the products mixed with the heated steam and fuel, resulting in simplified hardware and enhanced load-following ability.
One concept for an integrated steam/fuel reformer is shown in Figure 30.

7.3.3 Reformation of Natural Gas

Under equilibrium conditions, the reformation of natural gas (methane) with steam yields the product stream as listed in Table 17 where the operation temperatures are varied but the steam-to-carbon molar ratios of feed is kept at one-and-half. The steam/carbon molar ratio of 1.5:1 would translate to a steam/methane mass ratio of 1.6875. Thus for each pound of methane that comes into the system there would be 2.6875 pounds of the steam/methane mixture enter the reformer and generate 2.6875 pounds of the reformed product. Table 17 gives compositions and LHV calculated for the reformed product.

It should be noted that the LHV of the product reformed at 1300°F is 8737 Btu/lb but when allowance is made for the mass flow of 2.6875 lbs from 1lb of methane (LHV 21,520 Btu/lb), the heat content of the flow derived from 1 lb methane is 23,480 Btu.

The high-hydrogen gas formed is very advantageous from the point of view of combustion, as noted in the Introduction. It is desirable to maximize this content. Figure 31 shows a typical result for the steam-to-carbon ratio of 1.5 for various pressures within the reactor.

Table 17. Steam Reforming Products*

Steam / Carbon = 1.5				
Temperature (°F)	1200	1250	1300	1500
Composition (vol%)				
H_2	33.95	37.84	41.73	55.85
CH_4	23.32	21.04	18.62	9.05
CO	3.05	4.29	5.78	12.92
CO_2	6.20	6.24	6.10	4.27
H_2O	33.45	30.59	27.77	17.91
LHV (Btu/lb)*	8523	8623	8737	9299
(Btu/ft^3)	316	310	303	278

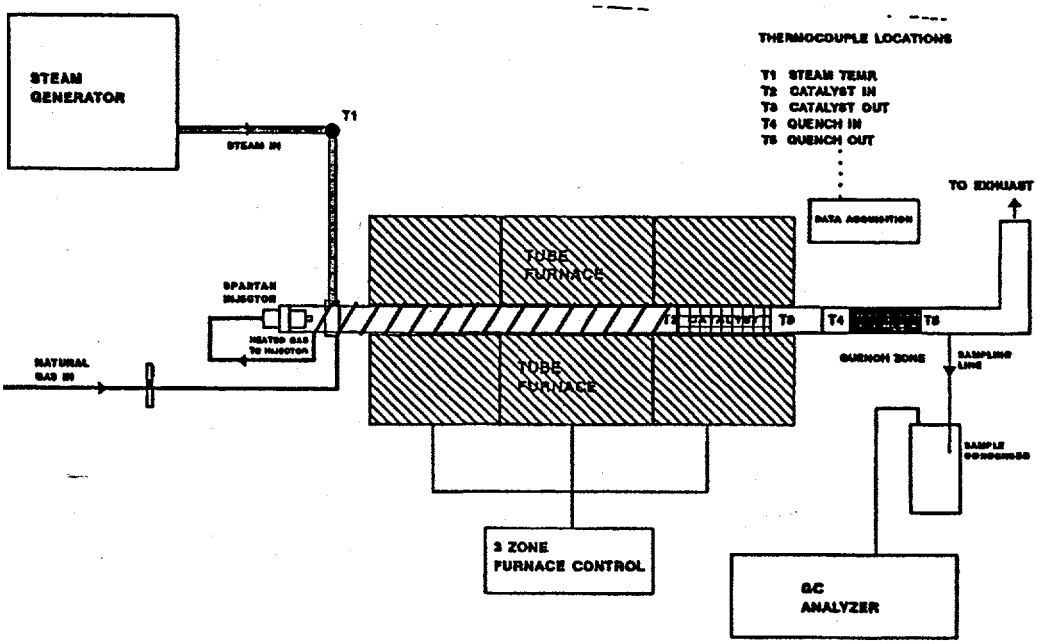

Figure 31. Tube Reactor for Reforming Catalyst Screening Tests

7.3.4 Catalyst Life

An effective fuel reforming catalyst requires the maintenance of a desired activity over its lifetime. Any known catalyst poisons or deactivators need to be carefully identified. Sulfur poisoning, catalyst migration, and substrate durability are contributors to the problems of catalyst life. The selection of a sulfur-tolerant catalyst is one of the critical material requirements for the processing of autothermal reforming Figure 32 shows the 36 inch long stainless steel tube reformer used to evaluate catalysts with natural gas feed. The gas composition was conventional with 92.8% CH_4, 4.2% C_2H_6 and 1 ppm S. Details of the equipment, control and measurement analyzers are given in Topical Report 8.3. Chromatographic analysis was used to measure the products of reforming.

Screening of catalysts was performed with a 1 inch diameter of monolith orfoam coated with the catalyst. Catalysts suitable for use in reforming must meet the dual requirements of high catalytic activity and sulfur poison tolerance. The level of catalytic activity dictates the hydrogen yield in the product stream. Candidate catalysts must meet these requirements with strong thermal stability. Two basic groups of reforming catalysts, nickel- and platinum-basis, were selected for the preliminary testing of the reforming activity. The tests were conducted at 1500°F and steam to carbon ratio of 1.34 under atmospheric pressure. All catalysts produced about 70% hydrogen (on a dry basis) in the product stream.

Reactant conversion and product distribution remained about constant during the 4-to-10 hours testing for both the nickel and platinum catalysts. No significant change in catalyst performance has been observed. Differences in activity of the nickel and platinum catalysts have been observed on the CO and CO_2 yields. The lanthanum promoted, nickel-based catalyst (DYCAT foam) converts natural gas to more CO instead of CO_2 and yields a higher heating value of product gas than other catalysts. There was no significant pickup of sulfur in any catalyst.

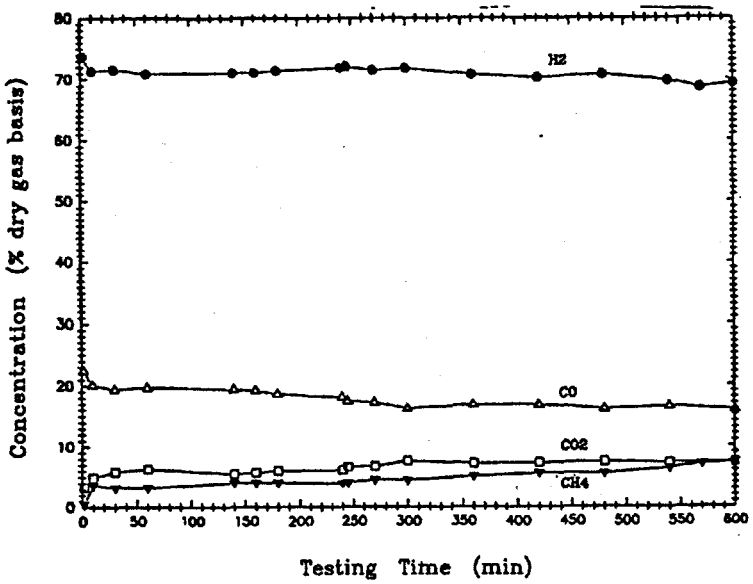

Figure 32. Product Distribution of Reforming Test With DYCAT Foam Catalyst

Figure 32 shows a typical plot of product concentration as a function of testing time. Over 70% hydrogen is generated within the first minute or so from natural gas.

An accelerated test of life was conducted with a methane doped with 200 ppm of hydrogen sulphide (H_2S) using another catalyst. No difference in performance was noted. Similarly EDX analyses showed no change in composition of the catalysts.

7.3.5 Reformation of Liquid Fuels

Use of a broad range of liquid fuels for industrial gas turbine operation has become an important requirement in power generation, marine service, and as back-up fuels for normally gaseous fueled installations. There is an increasing worldwide customer interest in the use of the more cost effective liquid fuels. However, the use of liquid fuels often has an adverse effect on gas turbine combustion and fuel systems. The liquid fuel's chemical composition, heating value, physical properties, and contaminations all must be addressed in order to meet specific system design requirements to ensure reliable operation. Small and medium size gas turbines having a relatively small nozzle throat area typically restrict any use of heavy liquid fuels. Even for large gas turbines, the engine must be shut down and washed from time to time to remove deposits when running liquid fuel.

The reforming of either gaseous or liquid fuels would produce the same primary constituents (with different proportions) regardless of the parent fuels. This would allow a single fuel injection and combustion system to be employed, thus making the system fuel independent to meet customer specified requirements. Dual fuel or even multi-fuel capability under the fuel reformation would broaden the market of the advanced turbine system applicability.

The lower hydrogen content of diesel fuel caused lower hydrogen and more CO in the reformed gas, and the heating values of the gas were higher than those found with natural gas. Typical results are shown in Table 18.

Table 18. Results of Liquid (Diesel) Fuel Reformation*

Reforming Catalyst Type	Nickel Basis			Platinum Basis		
Testing Time	5 min	314 min	405 min	15 min	380 min	522 min
Composition (vol %)						
H_2	62.2	63.0	60.9	65.2	64.3	64.7
CO	22.8	18.3	18.2	20.1	18.7	20.7
CH_4	5.6	5.6	6.5	4.6	6.2	5.1
CO_2	8.2	10.9	11.6	7.9	8.8	7.2
C_2+	1.2	2.2	2.8	2.2	2.0	2.3
Heating Value (Btu/lb) (LHV, dry basis)	9,495	9,429	9,368	10,260	10,242	10,511

*Reforming conditions: temperatures at 1500°F and steam-to-fuel (mass) ratio at 1.2.

7.3.6 Reformed Fuel (Hydrogen-rich) Combustion

One application of reforming liquid fuels will be to make ATS suitable for the transportation market. However, reformation of all fuels (with suitable clean-up) will be the improvement in combustion including reduction of NOx levels.

Hydrogen gas has by far the highest flammability ratio of 18.75, compared to 3.0 for natural gas (methane) or 4.52 for propane (as listed in Table 19). The flammability ratio of the fuel is defined as the upper flammability limit (UFL) divided by the lower flammability limit (LFL) which affects the range of combustor operation. Flammability limits directly influence combustor light-off, turbine cold/hot flameout and combustion efficiency during light-off and acceleration. Based on experimental and empirical data, a higher flammability ratio gives satisfactory gas turbine operation from start-up to full load, including load transients. The flammability ratio of the fuel depends primarily on the type and concentration of the individual constituents in the fuel. Hydrogen-rich gas generated via fuel reforming can help handle the engine start-up.

The hydrogen-rich reformed gas can extend the lean extinction limit to lower temperatures. This would allow the combustor to be operated in lean conditions for low NOx emissions. As shown in Figure 33, the limits of hydrogen flammability in air diluted with an inert gas is extended to the peninsula-shaped areas. No flame occurs only when the percentage of N_2 in air exceeds 75% or O_2 in the mixture is below 5.0%. For comparison, Figure 33 shows the limits of flammability of methane mixture in which the flammability range of methane is restricted below 38% N_2 or above 13 percent O_2.

Flame extinction with lean gases sets a lower limit to control of NOx levels with natural gas. The lowest temperature that can cause ignition for combustible substances varies greatly. The minimum ignition temperature for hydrogen or hydrogen mixtures is much lower than other gases. Light-off of the hydrogen-rich gas is relatively straightforward and requires no assistance of ignitor or pilot fuel. This reduction of system hardware is an important advantage of the hydrogen-rich gas combustion. The ignition energy of hydrogen is about 0.02 milijoule, which is less than 4% of the

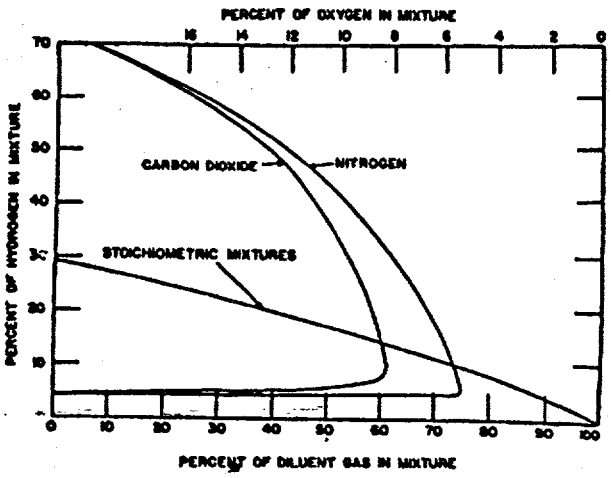

Figure 33a. Limits of Flammability of Hydrogen in Air Diluted With CO_2 and N_2

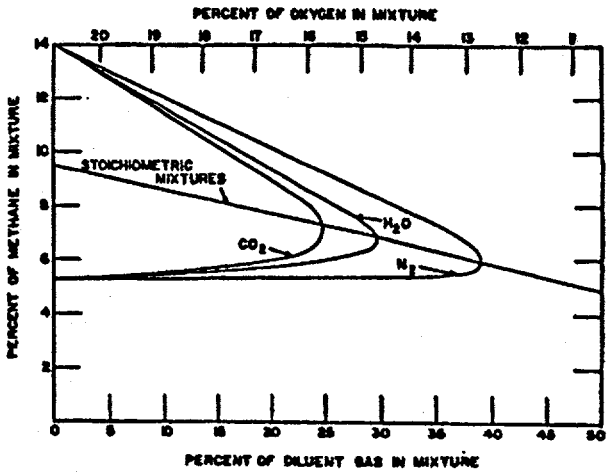

Figure 33b. Limits of Flammability of Methane in Air Diluted With CO_2, H_2O and N_2

Table 19. Flammability Limits and Flammability Ratio for Selected Gases (See Topical Report 8.3 for full list)

Gas	Limits of Flammability Lower	Limits of Flammability Upper	Flammability Ratio
Hydrogen (H_2)	4.0	75.0	18.75
Methane (CH_4)	5.0	15.0	3.00
Propane (C_3H_8)	2.1	9.5	4.52
Carbon Monoxide (CO)	12.5	74.0	5.92
Natural Gas (92.8% CH_4, 4.2% C_2H_6, 0.8% C_3H_8,)	4.9	15.1	3.08
Landfill Digester Gas (55% CH_4, 45% CO_2)	10.1	20.6	2.04

ignition energy required for natural gas (methane), a major factor in making low temperature catalytic combustion possible.

Several experiments were performed to demonstrate that the advantages with pure hydrogen fuel, (albeit diluted with selected gases) were realized with reformed gases. A comparison of non-reformed natural gas with partially and fully reformed gas, as well as with reformed diesel fuel confirmed that the advantages were retained. Topical Report 8.3 gives details of this portion of the work.

7.3.7 Integration with ATS

Demonstration of an integrated ATS system was beyond the scope of this critical technology evaluation. Nevertheless preliminary work was done to demonstrate the approach. Figure 34 shows how the integrated system would be assembled. Preheating of the water by the intercooler and by

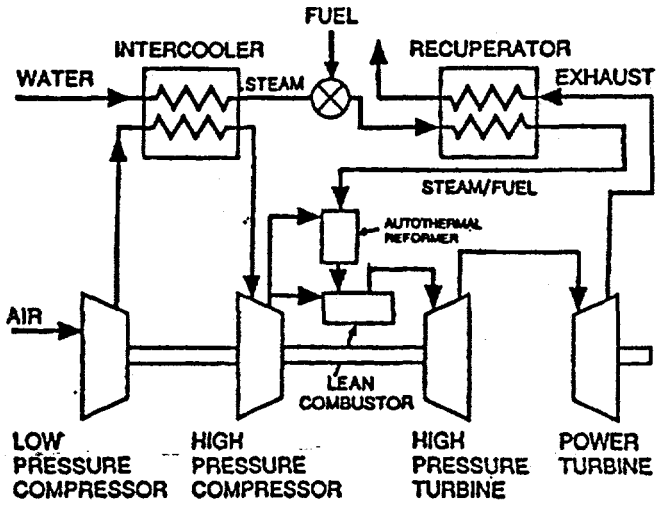

Figure 34. Integration of Fuel Reformer With Intercooled and Recuperated Gas Turbine

the recuperator to generate the steam/fuel gas mixture represents important energy savings.

A small pilot combustor in the autoreformer will provide additional heat for the fuel-steam mixture. The gases leaving the catalytic reformer will exit into the lean-burn, low NOx combustor to reach the desired inlet temperature for the turbine.

Some preliminary work has been performed to examine some of the critical aspects of the configuration shown in Figure 34. A sub-scale rich-lean combustor consisting of the reformer and selected catalyst was built and run. A fuel and steam mixture injector was designed and built. The first tests were conducted at 40 psig with reforming beds in the temperature range 1200-1500°F. A sub-sequent series was performed at 60-120 psig.

Smooth ignition and remarkably stable combustion were demonstrated at combustion temperatures up to 2500°F. Stable gas production was achieved. Control of the reformer bed temperature was not precise with a drift from 1300-1600°F.

The results were a very positive demonstration that the process is feasible. NOx emissions varied from 15 to 55 ppmv, but 15-30 ppmv are believed to come from the pilot combustor. Little or no additional heating is expected to be needed in a full size unit so that ultra-low NOx should be possible.

Details of these tests can be found in Topical Report 8.3.

7.4 HIGH TEMPERATURE TURBINE DISK

7.4.1 Problem Statement

Increasing the turbine disk rim allowable temperatures will permit blades and their attachments to run hotter, requiring less cooling flow, and resulting in greater cycle efficiencies. Boosting rim temperature above current levels would certainly require materials with better creep and stress rupture properties in both the blade attachments and disk posts.

The entire turbine rotor could conceivably be made from a cast nickel-base superalloy such as used in turbine blades which has the required rupture strength. However, cast superalloys typically have insufficient low cycle fatigue (LCF) strength for the bore region of todays 100,000 hour life designs. The goal of Task 8.4 is to develop a dual-alloy turbine disk which will satisfy the diverse property requirements of the rim and hub areas of the disk. The program examines methods of attaching a cast superalloy rim with optimized rupture strength to a fine grain hub material with improved LCF strength. The dual-alloy bonding demonstration is summarized in Section 7.4.3.

The rim temperature goals of the Dual-Alloy Disk Program coincide with a regime where superalloys typically exhibit a trough in rupture and tensile ductlities. It has been observed that the reduced ductility can be accompanied in some alloys by a tendency for notch sensitivity in rapture and an

adverse interaction between creep and fatigue when both deformation modes are operative. To address these issues, Task 8.4 examines advanced stress analysis and life prediction techniques for high temperature materials. The goal is to develop finite element analysis methods which more accurately account for material deformation and failure modes in the presence of mechanical notches. This effort was primarily directed toward analysis of the cast rim material and is summarized in Section 7.4.4. In addition, Task 8.4 explores Non-Destruction Inspection (NDI) techniques aimed at characterizing initial flaws in the disk structure and to monitor potential growth of cracks during cycle operation. NDI development is covered in Section 7.4.5.

7.4.2 Dual-Alloy Bonding Demonstration

Howmet Corporation was selected as the subcontractor for investigating bonding methods in demonstrating the Dual-Alloy concept. The Howmet Technology Center has valuable background in the bonding of cast superalloy materials for multi-wall blades and other structures. Solar and Howmet collaborated on all phases of the Program Plan, materials selection and process development. Early discussions with Howmet were to propose a cast rim with a hub section produced by Vacuum Plasma Structural Deposition (VPSD). This concept was subsequently abandoned because of size limitations (diameter) of the VPSD process, and the solid-to-solid concepts described in section 7.4.3.2 have been pursued.

7.4.2.1 Selection of Materials

Alloy Mar M 247LC was selected for the rim material of the Dual-Alloy disk. Mar M 247LC is one of the strongest equiaxed polycrystal alloys commercially available, and is an alloy which both Solar and Howmet have experience in blade and nozzle applications. Mar M 247 rim material was produced using Howmet's Spraycast process since it has the potential for being a lower cost alternative to investment casting, and also the product could be obtained in the time frame requied to support the program. Spraycast is a modified version of the OSPREY process in which vacuum melted material is argon gas atomized and spray formed directly into a ring shape. In addition to the Dual-Alloy application, spray casting technology has spin-off potential in the manufacture of other gas turbine ring shaped components since it can provide one or more of the following:

- Parts which cost less than those made from ring forgings.
- Parts from "unforgeable" alloys.
- Use of alloys providing creep strength not obtainable in forged alloys.

The hub material selected for the Dual-Alloy Disk Program is Udimet 720, a high strength nickel base superalloy available in wrought, forged and powder forms. In a fine grain-size condition Udimet 720 exhibits exceptional yield strength and LCF properties and is used extensively in aircraft and helicopter turbine rotors. The powder form of Udimet 720 was specified for this program because of its flexibility in processing and also because it was readily available.

7.4.2.2 Processing

Three processes were evaluated to demonstrate joining the Mar M 247 rim to the Udimet 720 hub. They were; (1) Diffusion bonding by Hot Isostatic Pressing (HIPing); (2) HIPing with surfaces 'activated' by boron deposits (boronizing); (3) Shear Forging. The first two were performed by Howmet and Shear Forging by Ladish Company.

Prior to process demonstrations, several preliminary studies were performed to obtain needed data to support process development. For example, single point machining trials were performed to assure the appropriate interface geometry could be obtained. It was found that single point machining left no carbide residue on the bond surfaces. Detailed surface roughness evaluations were performed to characterize the interface quality before bonding. Also, cleaning methods for preparing the surfaces for bonding were explored. Optimum boron levels for the boronized bond trials were established by examining HIPed sub-size specimens. 0.005 gms/sq. inch was found to give the best compromise between residual boron and porosity after HIPing at 2050°F under 15 ksi. Finally, heat treat and simulated HIP trials were performed to determine their effect on grain size of the hub and rim materials, then baseline mechanical properties were measured for later comparison to bonded properties.

Sub-scale 3.5 inch OD samples (2.0 inch hubs) were used for demonstration of the three bonding processes, all being carried in parallel. The initial desire for each bonding method was to maintain a maximum processing temperature below 2050°F in order to avoid grain growth in the Udimet 720 hub material. The first 4 shear bonding trials at Ladish at 2025°F were unsuccessful apparently due to lack of interface deformation and rounding/dulling of the molybdenum shear tool. It was recommended that the shear forge temperature be raised to 2165°F to enhance deformation, however, this did not result in bonding. Due to the unsuccessful subscale effort, the shear bonding task was canceled.

7.4.2.3 Solid-to-Solid HIP Bonding

The process which produced the best overall bond quality was solid-to-solid HIP bonding, and was therefore down selected for the remainder of the program. Further, this process was estimated to be the lowest cost of the three processes evaluated. Six 3.5 inch diameter prototypes were fabricated for process demonstration and bond line testing. Two HIP temperatures were evaluated; 2050°F and 2165°F. The six prototypes were delivered to OMI, Inc in Costa Mesa, CA for ultrasonic inspection of the bondline after HIPing but prior to solution and aging heat treatments. The inspection revealed no defects in 5 of the 6 specimens. One of the disks (specimen #5) showed indications of extensive debond. Review of records at Howmet revealed that this specimen experienced a rupture in the HIP can during the bonding process. It appears that the debond is related to this problem and the specimen was set aside. The five good prototype rotors were solution heat treated, rapid cooled and aged. The assemblies were again ultrasonic inspected at QMI and it appears that no heat treat related flaws were induced.

Radial bondline test bars were extracted from the five good prototype rotors for mechanical property evaluations. To date, a total of 33 elevated temperature creep-rupture and tensile tests have been completed. Metallographic examination revealed intimate bonding of the couple throughout the bond joint as indicated by the ultrasonic inspection. The two HIP cycles evaluated yielded different bond-line characteristics. A potential correlation between the degree of grain growth observed across the joint interface and bond quality/test ductility was observed. The 2050°F HIP processed couple showed a lack of grain growth and interdiffusion across the joint and tended to exhibit lower strain to failure and planar fracture surfaces. The 2165°F HIP cycle showed a greater degree of grain growth and better bond quality. Higher temperature and potentially longer time diffusion cycles are being evaluated to determine if they produce further interdiffusion and improved ductilities.

The conclusion thus far is that Dual-Alloy Rotors are technically feasible forindustrial gas turbines and the concept has been successfully demonstrated. The effort has pointed the way toward optimizing the HIP cycle and/or diffusion heat treatment efforts which are planned in Phase III to

improve bond joint ductility and properties of the rim/hub materials. The future effort will have the goal of producing bondline properties which meet the specific design of Solar's ATS.

7.4.3 Stress Analysis and Life Prediction

Stress analysis of the Dual-Alloy Rotor represents a significant challenge because of the high rotational stress and temperatures anticipated for the ATS engine application. Early in the Program it was decided to collaborate with Southwest Research Institute (SwRi) to develop the required approach based on their expertise in the field. A contract was awarded to SwRi to tailor existing codes and constitutive models, developed under EPRI, Nuclear and Aerospace Industry sponsorship, to the specific design aspects of the Industrial ATS. The effort was directed primarily at analysis of the blade attachment region of the disk, although it is anticipated the tools developed would be applicable to a broad range of high temperature components.

The program consists of 6 interrelated tasks aimed at analyzing the deformation modes in the area of mechanical notches and to apply creep-fatigue damage models calibrated to the disk rim material, Spraycast Mar M 247. Data have been generated to support the model including uniaxial tensile and cyclic stress-strain response, low cycle fatigue, creep-rupture life and ductility, notch sensitivity behavior, constitutive law parameters and creep stress relaxation data. The goal is to deliver a recommended constitutive relation to be used in non-linear, time-dependent stress analysis. Solar provided SwRi with the design and stress inputs required to proceed.

Several preliminary observations have been made based on the body of tests completed including: 1) The spraycast process resulted in a very fine grain (and somewhat non-uniform MAR M 247) structure relative to the goal, which in turn has impacted the creep-rupture performance. Howmet's attempts to coarsen the structure by varying spraycast parameters were unsuccessful. 2) The spraycast Mar M 247 has exhibited notch sensitive behavior at certain temperature/stress conditions. Because of these factors, a coarser grain equiaxed version of Mar M 247 is being considered for ATS Phase 3 using the same bonding method.

The final conclusions for the stress analysis and life prediction effort will be reported in the Topical Report based on all of the testing inputs and review of the constitutive law parameters.

7.4.4 Non-Destructive Inspection Development

A non-destructive inspection technique based on eddy current has been developed for finding flaws in blade attachment slots in the turbine disk. Inspecting the slots in the past has been difficult by visual or Fluorescent Penetrant Inspection (FPI) because of poor access in the confines of the long axial length of the slots. Eddy current probes have the potential for high sensitivity without the access limitations. This capability will be important for monitoring potential growth of cracks during cyclic operation of the ATS turbine disks. The development task was performed under a subcontract to the NDE Applied Research Department at Southwest Research Institute.

The Program has successfully integrated a small diameter eddy current probe into a fixture, or carrier tool, which is passed manually through the disk slot. Inspection standards have been fabricated using a range of EDM slots in the trial disk material, Alloy V-57. Alloy V-57 was selected to demonstrate the concept since Solar has existing turbine products with significant engine hours for experimentation and inspection. A deliverable of the Program is a detailed inspection technique for the process. It is based on characterizing the known EDM slots in the eddy current standard and calibrating the equipment frequency and sensitivity for the specific material and geometry. The

technique was completed by SwRi using eddy current equipment and personnel from Solars Desoto facility, thus making the method easily transferrable to turbine overhaul and/or production.

Two turbine disks were randomly selected from the turbine overhaul cycle for an initial demonstration. The disks received two eddy current inspections, one prior to grit-blast cleaning of the slots and one after cleaning. Prior to cleaning one of the disks had numerous reportable indications when inspected. However, after cleaning the indications were no longer detectable. It appears that surface condition is an important variable and that cleaning prior to eddy current inspection will be required. This will be incorporated into the inspection technique sheet. Additional turbine disks with high operational hours are available and are planned to be inspected in the follow-on Phase III effort. We are also evaluating the possibility of using ultrasonic inspection of the cracked structures since in this method the turbine blades would not have to be removed during inspection. Cracks which are found in the experiment will be sectioned open in the laboratory for dimensional analysis and further calibration of the non-destructive inspection techniques.

7.5 FULL SCALE, SINGLE CAN CATALYTIC COMBUSTOR RIG

This work constituted WBS 2.8.5 on the ATS Program. Topical Report 8.5 should be consulted for more details of this work.

7.5.1 Introduction

This subtask was added by revision A003 to the contract and was originally titled "Low emissions combustor". As part of an overall catalytic combustor project along with Subtask 8.2, it is now defined as catalytic combustor development using a full ATS scale single can rig.

It was planned that the catalytic combustor design being developed at the subscale level as described in Section 7.2 would be tested in a single-can, full-scale combustor rig. However, the development work described in Section 7.2 did not progress as rapidly as planned although much valuable technical information was generated. The latter was essential to achieve stable operation of a catalytic combustor at low emissions. The work in the earlier task allowed a design to be completed ready for test in Phase III.

7.5.2 Design of a Full-Scale, Single Can Combustor

The combustor diameter was increased to approximately 10 inches. The system was designed to be representative of the full-scale engine design including a premixer, catalyst bed, post-catalyst combustor and an integral part-load injector situated along the centerline of the cylindrical combustor. The combustor will be operated over the full range of engine operating points including simulated start-up, idle, low load, and catalytic mode over 50-to-100% simulated engine load. System performance will be characterized through measurements of emissions, pressure loss, catalyst bed temperatures, and combustor exit temperature profiles. Catalyst beds will be supplied by Engelhard corporation based on their designs being developed during subscale testing. This effort is an important step in advancing catalytic combustion to engine readiness.

The basic design of this rig was completed but was placed on hold in order to allow for the detail design to accommodate changes indicated by the subscale rig test work of Subtask 8.2. Primarily these changes relate to continuing development of fuel injection methods for obtaining satisfactory catalyst inlet velocity and fuel/air mixture profiles and to providing sufficient post-catalyst volume to enable CO burn out to <10 ppmv levels. These features have been defined and incorporated into

the rig which has completed fabrication and assembly. The rig is now on a short hold for its designated test cell to become available for its installation and test in Phase III.

7.6 TOTAL PLANT CONTROL

This work constituted WBS 2.8.6 on the ATS program. Topical Report 8.6 should be consulted for more details of this work.

7.6.1 Introduction

Solar has operated a gas turbine remotely for many years. For example, three unattended 9 MW Solar generator units were installed recently in the Northern Territories of Australia and controlled from Darwin, over 100 miles away. Such operation requires both an extremely high degree of reliability but also requires flawless control systems. It is the latter that Solar recognizes as essential for market penetration, especially in distributed power generation, as in Northern Australia. The standards attained it the past must be equaled or surpassed with the more complex, low emissions ATS.

The new standards will require improvements in gas turbine control systems in order to fully support ATS goals. Such control systems require that a Man-Machine Interface (MMI) operate within a multi-tasking, multi-user environment. Design and demonstration of such a system was undertaken to include advanced human interface features, advanced networking capability, the employment of expert systems, and low-cost, long-range communications capability. The systems will provide for easy customization to customer's unique requirements as well as for simple in-the-field reconfiguration.

Initial efforts entailed configuring Solar's Systems Engineering computers to work with the software required in developing the MMI. Writing of a design specification for the MMI was completed early in the program.

Next, the development operating system hardware and software were procured and installed. The ATS development Application Server sub-network was installed along with developer workstations for executing the proof-of-concept task. This equipment has been tested and the development of communication protocol established between the Allen Bradley PLC and MMI. Specification for software development standards have been prepared.

The MMI data acquisition module was developed for the incumbent hardware, an Allen-Bradley microprocessor and the MMI test work station installed. Initial real-time meters routines, windowing techniques and real-time trending routines were developed. An initial database was constructed from MMI descriptors, scaling and memory identification. The latter includes routines to retrofit existing display systems.

The proof-of-concept has been demonstrated based on the design specification. In addition to the data acquisition module for an Allen-Bradley Programmable Logic Controller (PLC), another is being developed for a Modicon PLC. During the proof-of-concept phase, it was determined that the system resources required by the Graphical User Interface (GUI) would not allow some of the functions required for the ATS application. Alternate GUIs were evaluated.

7.6.2 Design Work - Prototype

The MMI issue was of increasing importance as prototype work was begun. The MMI ergonomics were reviewed with a human factors consultant and the Windows NT operating system was examined as an alternate to the UNIX operating system. A detailed comparison was made of the two systems but deciding factors were the ready acceptance of Window NT in Solar's marketplace and better software development tools than UNIX.

A specification for a prototype was developed. The prototype will demonstrate the look and feel of the overall system as well as some of the advanced features. Work in this step was guided by a project plan to guide the team and ensure inclusion of all requirements in the prototype.

Acquisition of all components and construction of the prototype for test work was completed.

7.6.3 Detailed Design Specifications

Completion and a test of the prototype led to work on a detailed specification. This document will serve two purposes. Initially, the composition of the system will provide a map of the design and development efforts required for the complete system. This will then be used in developing the project phases and plan. Secondly, the design Specification document will be the repository for the detailed designs of each of the modules, processes, and data elements that make up the system. Previous design information for the UNIX-based system will be integrated into this document as appropriate. Further this document will provide the transition from work in Phase II to the demonstration in Phase III.

7.7 HIGH TEMPERATURE RECUPERATOR MATERIALS

This work constituted WBS 2.8.7 on the ATS program. Topical Report No. 8.7 should be consulted for more details of the work.

7.7.1 Introduction

Section 7.1 of this report describes work on the Low Pressure Drop Recuperator. This critical technical requirement for ATS was met by Solar's Primary Surface Recuperator (PSR) substantiated by nearly 2 million hours of field service with individual units having nearly 50,000 hours of operation. The intercooled and recuperated ATS discussed in selection of Gas Fired Advanced Turbine System (GFATS) will require higher pressure ratios and higher temperatures for the recuperator than those demonstrated in prior service of the PSR. For these advanced cycles, materials of high creep strength, high yield strength and oxidation resistance are required, and for some cycles, or expensive alloys, such as Inconel 625 or Haynes 230, may be needed.

The primary failure mechanism for the PSR has been creep. Unfortunately, there has been a general lack of validated creep data for the thin foils that are the primary component of solar's PSR. Therefore, a systematic study was undertaken to fully define the operating lines of various thin foils, including SS-347, Inconel 625, and Haynes 230.

Development of a PSR material with greater temperature capability will provide two future improvements to Solars ATS:

- With the advent of turbine airfoil material and cooling technologies that will allow design point firing temperature (TRIT) to be increased, cycle efficiency can be thus

improved without the need to increase overall pressure ratio to maintain the present recuperator inlet gas temperature.

- At any given design point temperature, higher off-design (part load) temperatures can be scheduled in order to provide improved part load overall efficiency. This will improved the competitive position of the ATS against natural gas-fueled piston engines which can demonstrate a very flat part load efficiency curve. The variable area nozzle (VAN) in the ATS power turbine is the enabling feature for this plan.

A list of the candidate materials to meet these varied demands is given in Table 20.

Table 20. Recuperator Alloy Candidates

Material Class	Material
Iron/Chromium/Nickel alloys	347 Stainless steel
	RA 85H
Iron/Cobalt based	N-155
Nickel/Chromium and Nickel/Chromium/Iron alloys	Inconel 600
	Incoloy 800
	Incoloy 825
Nickel/Chromium/Molybdenum	Inconel 625
	Hastelloy-X
Nickel/Chromium/Tungsten/Molybdenum	Haynes 230
	RA-333

Another critical requirement is affordability. Materials such as Haynes 230 or Inconel 625 typically cost four times as much as the currently used Type 347 stainless steel. Manufacturing cost thus dictates that these materials be used only in that portion of the recuperator that is actually exposed to high temperature and continuing with Type 347 where the temperature has been reduced by the extraction of heat from the exhaust gas.

7.7.2 Tensile Tests

Full details of the tensile test data can be obtained from Topical Report 2.8.7. Figure 35 shows some typical results for the yield strength versus temperature of Type 347 stainless steel. Individual data points are shown together with the lower bound at 95% and 99.5% confidence levels. Details of results are in the Topical Report. One problem of potential importance was reproducibility. Figure 36 shows the tensile yield of 153MA. The large amount of scatter gives a very low value for the lower limits of confidence. Figure 37 compares the tensile yield strengths at the lower 99.5% confidence levels.

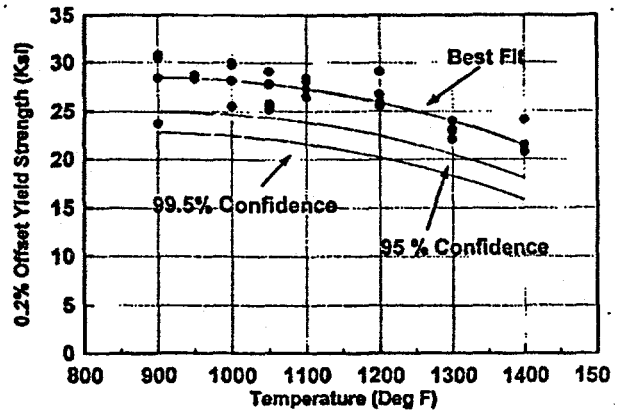

Figure 35. Yield Strength vs. Temperature T347 SS (0.0035 in. Foil)

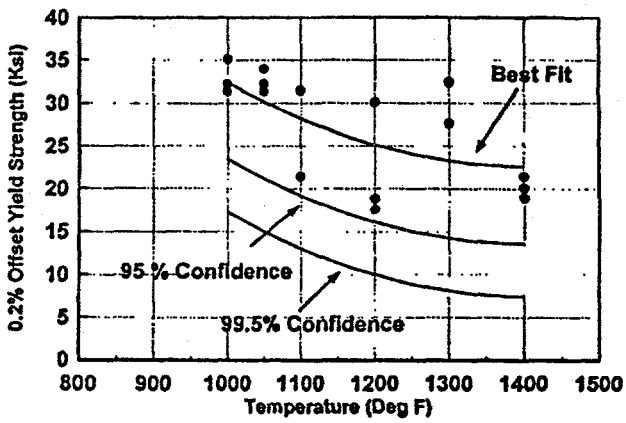

Figure 36. Yield Strength vs. Temperature - 153 MA (0.0035 in. Foil)

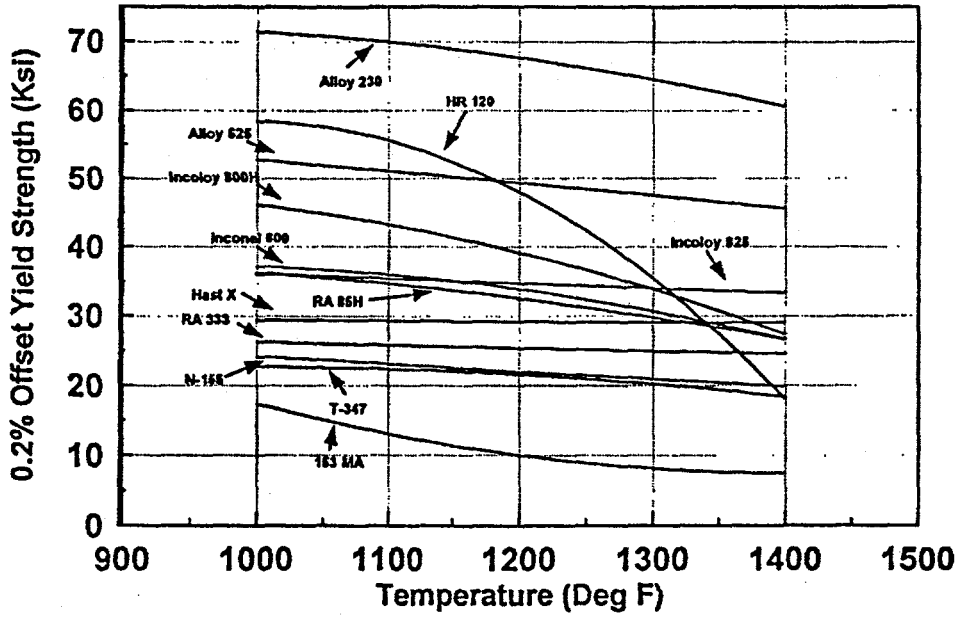

Figure 37. Yield Strength vs. Temperature for Various 0.0035 in. Foils (99.5% Confidence Range)

the wall of a cell is smaller than this test area used and creep failures are known to occur locally. The low values of the lower bound of yield strength of 153 MA at 99.5% confidence makes this material an undesirable candidate that might increase the probability of local creep failure.

7.7.3 Oxidation Tests

Oxidation tsts were started but these were long time exposures and will be carried forward into Phase III. A key question is how to predict a life of 100,000 hours using tests that may not extend beyond 10,000 hours.

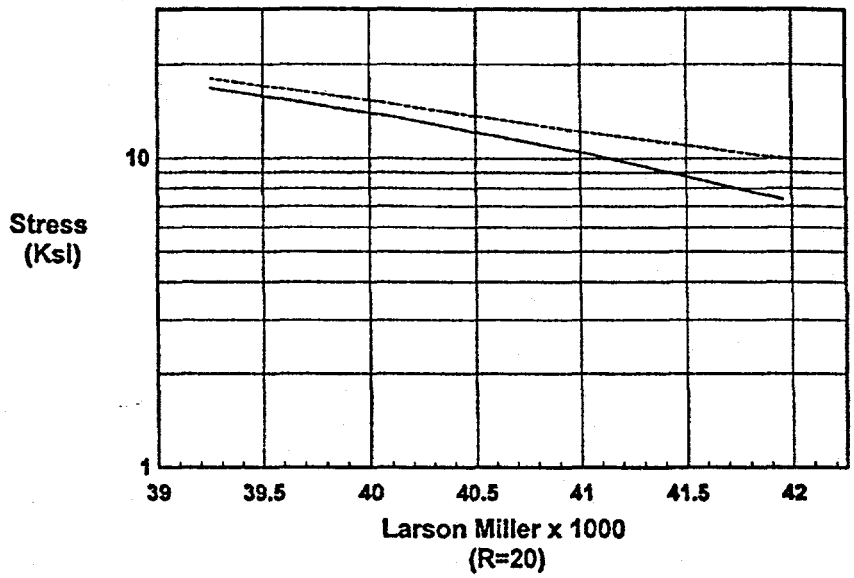

Figure 38. Type 347 Stainless Steel Stress Rupture

7.7.4 Creep Tests

The high pressure ratio cycle will increase the stress on the foils in the PSR, so that creep resistance became a more important requirement.

It was recognized that published data on creep, measured on bar or sheet, might not be valid as a design guide for foil. Some of these differences include: (1) typical grain size of foil is ASTM10; (2) long term creep is accompanied by a change in composition as active elements such as chromium are transferred from the alloy to the oxide; and (3) there is a loss of cross section as oxidation proceeds. For these reasons it was clear that data needed to be established on this program. Figure 38 shows the difference found between published values for wrought material and stress rupture results determined in this work for 0.0035 inch Type 347 stainless steel foil.

Creep test work was performed at both Solar and at Westmoreland Mechanical Testing and Research Inc. Repeated comparisons showed no systematic difference and no differentiation will be made. Topical Report No. 8.7 includes details of all tests.

Creep test temperatures ranged from 1250°F to 1480°F. Stresses were selected to give failures in 100 hours or more. Tests were run for as long as 4400 hours but were stopped prior to this in the event of failure or of more than 5% creep. Evaluations of recuperators returned from the field and analysis of foil creep and recuperator pressure drop combined to indicate that 5% creep might be a maximum practical limit.

7.7.4.1 Type 347 Stainless Steel

Twenty-five creep tests were conducted on foils of the basic recuperator alloy in thicknesses between 0.0025 inch and 0.0032 inch. Both longitudinal and transverse orientations were tested. The 5% creep point was reached in 670 hours at 1225°F under 17 ksi or at 1300°F under 12 ksi.

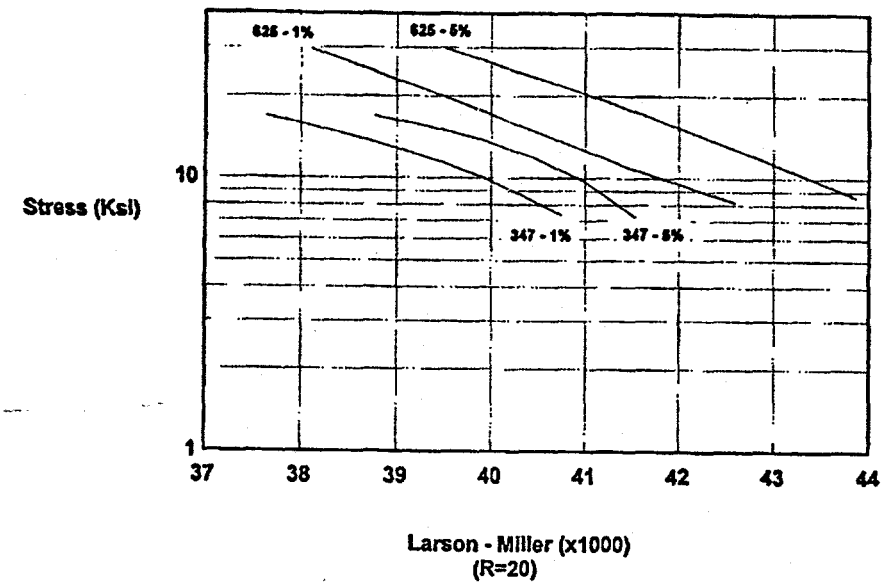

Figure 39. Stainless Steel Type 347 Thin Foil Test Results - Larson-Miller Curves

7.7.4.2 Inconel 625

Fifteen creep tests were conducted on foils of this potential candidate for an advanced PSR. The 5% creep point was reached in 670 hours at 1275°F under 30 ksi (at this temperature, Type 347 will withstand approximately 14 ksi so that Inconel 625 has at least twice the creep strength of Type 347).

7.7.4.3 Other Alloys

Data was gathered on 10 other alloys. Reference should be made to Topical Report No. 8.7 for details of all of the results.

Figure 39 shows typical results for foils of Type 347 and Inconel 625 for creep to 1% and 5%.

7.7.5 Other Work

A concept to use a dual alloy sheet was explored. Both EB and laser edged-welded (Type 347 stainless steel to Inconel 625) samples of recuperator foils were supplied by Belt Technologies, Inc. These samples were then successfully folded into finned recuperator sheet stock at Solar's recuperator manufacturing facility.

Laser welded and electron beam welded bi-material sheets, which were successfully folded, have gone though the required edge rushing tests without any problems at Solar's recuperator manufacturing facility at Morton Metalcraft. Visual inspection and metallographic examination revealed no flaws or cracks in the weld or adjacent regions. The crushing operation is the most difficult forming operation in the cell manufacturing process. Therefore, this success is a strong indication that the concept will be viable from a fabrication standpoint. A series of tensile tests of the welded couples were also completed this period, with very encouraging results. The concept will be carried into Phase III to evaluate the economics of scaling-up a production system.

Modified type 310 stainless steel being developed by Oak Ridge National Laboratories (ORNL) offers the possibility of adding about 50°F to the temperature capability of Solar's primary surface recuperator over that of Type 347 stainless. This capability will then exist within a cost range typical of stainless steels rather than at the much higher cost of nickel-based alloys.

Prototype samples of Modified 310 Stainless Steel were received from Oak Ridge National Labs. The material was cold rolled by ORNL to 0.020 inch thick for preliminary evaluation of microstructure and tensile strength. The tests at 0.020 inch gage thickness will form the basis for a decision on materials to carry into Phase III as thin foils.

7.8 LOW COST CERAMIC MATERIAL

This work constituted WBS 2.8.8 on the ATS program. Topical Report 8.8 should be consulted for more details.

7.8.1 Introduction

This subtask was originally titled "Reheat Combustor Material" and was proposed in anticipation of future addition of a reheat combustor to the ICR gas turbine cycle. With the emphasis on the optimized recuperated cycle, the goal of the subtask was changed to the evaluation of materials suitable for use in gas turbine combustion liners. It now supplements similar work being conducted by Solar under DOE Contract No.DE-AC02-92CE40960, titled "Ceramic Stationary Gas Turbine (CSGT) Development". The use of ceramic combustor liner in gas turbines contributes toward emissions reductions by freeing cooling air for use as primary combustion air and by allowing higher wall temperatures which contribute to the more complete combustion of hydrocarbons.

Information from a literature's survey, manufacturer's data, and Solar experience was used to select three materials for testing. In addition to material properties requirements for selection, subscale combustor liner cost was required to be at least half the cost of the same liner made from high modulus continuous fiber reinforced composites. The three materials initially selected for evaluation are listed in Table 21. Four hour subscale rig tests were planned for eight inch diameter liners made from each material. Upon successful completion of each four hour test, a fifty hour test was planned.

Cyclic thermal/erosion testing at ITP was also planned for comparative analysis of different fiber blends in the Altra KVS material. The test apparatus consists of a gas burner that automatically cycles on and off for 695 cycles per day. Test specimens are soaked to about 2350°F (1288°C) at the end of the test cycle.

Table 21. Candidate Ceramic Materials for the Combustor Application

Material Name	Type	Supplier
B-30	BZP	LoTEC
Altra KVS 16	high alumina fiber reinforced composite	International Thermoproducts
System 22 High Temperature Composite	glass-ceramic fiber reinforced composite	AEA Technologies

7.8.2 Modification of Program

AEA Technologies, formerly a U.K. government organization, was privatized after being selected for participation in this program. After reorganizing, they were unable to use their subcontractor for HIPing the System 2.2 glass ceramic composite in the eight inch subscale combustor size. Therefore, AEA Technologies was dropped from the program, and a relatively low cost Nextel 440 fiber reinforced glass-ceramic composite from Scientific Applications International Corporation (SAIC) was chosen as a replacement (CMC-SAIC-8).

7.8.3 Coordination With the CSGT Program

The CSGT program has tested 8-inch subscale combustor cans of silicon carbide composite (SiC/SiC) from DuPont Lanxide Corp. and B.F. Goodrich Aerospace as well as aluminum oxide (Al_2O_3/Al_2O_3) cans from Babcock & Wilcox. The three materials selected for evaluation in subtask 8.8 were as follows:

- B-30 BZP (Barium Zirconia Phosphate) supplied by LoTEC. This material features a zero coefficient of thermal expansion, eliminating all thermal stresses, and the potential to reduce the $30,000 per can cost of SiC/SiC material by 94%.

- CMC SAIC-8 (Nextel 440/Al_2O_3 -SiO_2) offers the toughness and strength of a CFCC material at a cost 60% lower than the that of SiC/SiC. This material is supplied by SAIC.

- Altra KVS 16 (Al_2O_3 fibers/Al_2O_3 - SiO_2) from International Thermoproducts with temperature capability to 3000°F at a cost 90% lower than that of SiC/SiC.

7.8.4 Coordination With ATS Phase III

The LoTEC liner and the SAIC liner were both tested in February in Solar's high pressure single can subscale rig. This facility has the capability to achieve engine rated pressures and temperature while maintaining a single injector's mass flow into the rig. It is fully instrumented for temperature, pressure, flow, and emissions measurement.

Each liner was instrumented with fifteen thermocouples attached to the outside with an alumina based adhesive. The thermocouples were arranged in three axial rows of five. Axial and circumferential spacing were about 1.25 inches and 120°, respectively. Nextel 440 is used to insulate the liner and as a compliant layer between the ceramic liner and the metallic housing of the rig.

In the BZP test, the rig was lit successfully, and heat-up to the target wall temperature of 1925° (1052°C) was started. However, eight minutes into the test, the liner failed catastrophically. One of the thermocouples was exposed to the combustion gases, overtemped, and caused an automatic shutdown of the rig. Post-test examination of the liner pieces indicated that the liner probably failed from thermal shock. Also, the fracture pattern suggested that failure originated from a large inclusion in the material.

The SAIC liner was lit successfully, but failed catastrophically about nine minutes into the test. Maximum wall temperature upon shutdown was 1995°F (1091°C). Post-test evaluation revealed that the composite exhibited extremely brittle failure with no fiber pullout, and the material was easily broken apart by hand. The fracture pattern was indicative of thermal shock.

The ITP liner will be instrumented using the same pattern as the other liners and will be tested in early May. This material is a refractory rated to 3000°F (1649°C). It is much softer than the other materials, but a proprietary method has been used to increase its erosion resistance for the combustor application.

To qualify this material in terms of erosion and thermal shock resistance, thermal cycle testing is being performed by ITP. They are currently testing two fiber blends, one rated at 2300°F (1260°C) and one rated at 3000°F (1649°C). Both are being cycled about every two minutes for 695 cycles per day. Natural gas is being used to heat the samples to between 2200°F (1204°C) and 2400°F (1316°C). Cold cycle temperatures are estimated to be between 600°F (316°C) and 800°F (427°C). Both samples have over 17,000 cycles and show no evidence of surface cracking or wear. The implication from these results is that the lower cost 2300°F may be sufficient for the combustor application.

7.9 ADVANCED CERAMIC MATERIALS

This work constituted W.B.S. 2.8.9 on the ATS program. Topical Report 8.9 should be consulted for more details.

7.9.1 Introduction

Advanced ceramic materials such as CFCCs have shown good promise on the companion program entitled Ceramic Stationary Gas Turbine (CSGT). In particular, CFCCs appear to have more promise than monolithic tiles in structural integrity as a combustor. Also, the CFCCs have provided the improved performance required for the ATS combustor. The demonstrated advantages on CSGT justified work to explore the use of advanced ceramic composite materials in other gas turbine components. Sub-tasks included development of a suitable (cost-effective) component fabrication process, the development of a finite element stress analysis to assure 30,000 hours of component life and the actual fabrication of a demonstration article.

The majority of the task has been subcontracted to the Supertemp Division of B.F. Goodrich Aerospace. Materials considered are both carbon-reinforced silicon carbide (SC) or silicon carbide-reinforced silicon carbide (SiC/SiC).

7.9.2 Selection of Components

Initially, components considered for development in this material included a turbine interstage duct and a power turbine blade. Applicability of ceramic composite materials in these components was more significant in an ICR gas turbine than in the optimized recuperated power plant. The final component selected was the transition duct between the combustor can and the stage one turbine annulus in the recuperated gas turbine.

Work started on this component in July 1995. A Pro-E computer model of the duct was completed by Solar. This was reviewed by BFG. Solar and BFG iterated on the design to arrive at final dimensions for fabrication.

A hard copy drawing of the combustor duct was delivered to BFG after agreement on the design along with its electronic model. The Brecksville Division of BFG is currently performing a stress analysis of the duct.

Tooling design was underway at the end of Phase II.

7.9.3 Coordination With ATS Phase III program

The results of this work on tooling, process development and life prediction for this class of material will be carried forward to Phase III of the ATS program.

Section 8

GLOSSARY

ACE	Advanced Component Efficiency. A Solar-funded multi-disciplinary, advanced technology program. It currently includes programs on compressors, turbines, cooling, and ducting.
ATS	Advanced Turbine System. A gas turbine-based energy conversion system as defined To the U. S. Congress by the U. S. Department of Energy (DOE). An ATS is distinguished from current gas turbines by markedly increased thermal efficiency, reliability, availability and maintainability and by decreased exhaust emissions and cost of power produced.
ATS50	Solar's designation for an ATS designed to meet the contract goal of 50 percent thermal efficiency.
ATS60	Solar's designation for an ATS designed to meet a "stretch" goal of 60 percent thermal efficiency.
BASELOAD	Typically describes a specific number of operating hours the power generation system is operating. In this case it represents (on average) 6500 hours.
BZP	Barium Zirconium Phosphate. A family of materials whose composition can be tailored to result in low, or zero, coefficient of thermal expansion. It is resistant to thermal shock, and is stable to 1200°C.
CFATS	Coal-Fired Advanced Turbine System. An advanced turbine system modified to operate on coal or coal derived fuel.
CFCC	Continuous Fiber-Reinforced Ceramic Composite. A high temperature composite material which consists of a ceramic matrix reinforced with fabric, tape, or rows of a high modulus fiber. CFCC's are typically not as flaw sensitive as monolithic ceramics, and can be fabricated into large parts such as combustion chambers.
CHORD	The axial length of an airfoil measured along a line drawn tangent to the leading- and trailing-edge radii. Chord is the characteristic dimension used in scaling of airfoils.
CSGT	Ceramic Stationary Gas Turbine. A DOE-funded program contracted to Solar Turbines Incorporated. The program goal is to demonstrate improved performance of a production gas turbine by retrofitting key components with ceramic counterparts for a 4000-hour field test.
EDX	Electron Diffraction Xray.

EFFECTIVENESS	(ϵ_R for recuperator, ϵ_I for intercooler). A characteristic of a heat exchanger – the ratio of the amount of heat transferred to the total heat available in the hot fluid between its entry temperature and the entry temperature of the cold fluid.
EFFICIENCY, COMPRESSOR	(η_c). Ratio of the work imparted to the air flow to the total work input. Unless otherwise specified, "adiabatic" efficiency (subscript. - ad) is implied, i.e., flow conditions at both inlet and outlet are in terms of absolute, or total, pressure and temperature. "Polytropic" efficiency (subscript. - p) is the theoretical efficiency of a very large number of identical low pressure-ratio stages and essentially normalizes pressure ratio for comparison of differing compressors.
EFFICIENCY, THERMAL	(η_{th}). Also termed cycle efficiency. The ratio of energy input to energy output from a gas turbine. Unless specifically designated otherwise, thermal efficiency of an ATS will be defined on the basis of net power output from the turbine shaft.
EFFICIENCY, TURBINE	(η_t). Ratio of the work produced by a turbine to the work it extracts from the gas flow. When applied to a GP turbine, total-to-total efficiency is implied, this definition being based on total or absolute inlet and exit conditions. When applied to a power turbine, total-to-static efficiency is implied, thus accounting for static pressure recovery as a result of kinetic energy conversion in the exhaust diffuser.
FGM	Functionally Graded Material. A multi-layer material or coating system with each layer graded to provide different properties at the surface of the component relative to the core or substrate. An illustrative example would be a turbine tip-shroud with a top coating tailored for abradability, an intermediate layer designed for oxidation resistance, and a substrate tailored for high strength.
GAS PRODUCER	(Abbr. GP) An element, or module, of a gas turbine which is required to provide a hot gas stream capable of propelling a power output turbine or other energy conversion device. As a minimum it consists of a compressor, a combustor, a turbine and associated shafting. Each of these components, in turn, may be of any of several types and may consist of one or more stages.
GPT	Gas Producer Turbine. May include HP and LP turbines.
GFATS	Gas-Fired Advanced Turbine System. An advanced turbine system which uses natural gas for fuel.
GP	See GAS PRODUCER.
HCF	High Cycle Fatigue. High cycle fatigue is characterized as the fatigue mechanism where vibratory loads are superimposed onto a steady state loading condition. The typical example is turbine blade under aero excitation. The turbine blade exhibits a significant steady state stress level due to the centrifugal load, where vibratory stresses are induced by high

	frequency pressure perturbations in the gas stream. Vibratory stress levels are typically within the elastic range of the materials. Failures typically occur due to excitation at the component's natural frequency, setting up a resonant condition. This failure mode is associated with large numbers (10e5 - 10e7) of low stress amplitude cycles.
HIP	Hot Isostatic Pressing. A process for simultaneously heating a component, or powder metallurgy compact while subjecting it to isostatic pressure using an inert gas atmosphere. The temperature and pressure area are high enough to produce densification of the materials.
HP	High Pressure. This prefix is used to designate an individual section of a series pair of aerodynamic components operating in the high pressure regime of the two. HPC designates the high pressure compressor and HPT designates the high pressure turbine of an HP, or high pressure, spool.
INTERCOOLER	A heat exchanger placed between stages of compression in a gas turbine in order to remove heat from the compression air thereby reducing the temperature of air going to and through the succeeding stage(s).
I.O.U.	Investor Owned Utility. There are approximately 260 investor owned utilities in the United States. They are differentiated by the fact that they are owned through a stock ownership plan and are usually traded on the open market. they are more tightly regulated in their service area by regulatory bodies like public utility commissions than the Municipal utilities or the cooperative utilities.
IPP	Independent Power Producer. A non-regulated producer of electric energy. Currently the majority of these IPPs are larger power generation stations much like the Central Power Station that is owned by the Investor Owned Utilities.
LAC	Levelized Annual Cost. The name of the financial model used by the utilities to determine the cost of the capital equipment of the usable life of the equipment. Takes into consideration present worth arithmetic. Sometimes interchanged with book value analysis/life cycle analysis.
LCF	Low Cycle Fatigue. The fatigue mechanism typically associated with large thermal or mechanical loading. The cycles are typically a transient loading condition, such as start-up and shut-down of an engine. Low cycle fatigue is characterized by allowable pseudo elastic strain range for a material whereby a fatigue crack will develop after a specified number of cycles. typically LCF is considered cyclic loading of the base load leading to plastic deformation. Cycles are on the order of less than 10,000 to 15,000 cycles.
LP	Low Pressure. This prefix is used to designate the individual of a series pair of aerodynamic components operating in the lower pressure regime of the two. LPC designates the low pressure compressor and LPT designates the low pressure turbine of an LP, or low pressure, spool.

McrAlY — A designation for an overlay coating applied to superalloy turbine components for increased oxidation and corrosion resistance. "McrAlY" is derived from the elemental constituents of the coating i.e., Cr = Chromium, Al = Aluminum, Y = Yttrium M = Ni Fe or Co (depending on substrate).

NEPA — National Environmental Policy Act.

PATTERN FACTOR — (Abbr. PF). A parameter defining the range of temperatures extant in the exit gas flow from a gas turbine combustor.

$$PF = \frac{T_{MAX\ EX} - T_{AVG\ EX}}{T_{AVG\ EX} - T_{AVG\ INLET}}$$

All temperatures are absolute.

PF — See PATTERN FACTOR.

PITCH — The circumferential distance between two adjacent airfoils in an axial turbomachinery annulus. It is equal to 2 times pi times the radius from the annulus centerline to the subject airfoil divided by the number of airfoils in the annulus.

POWER TURBINE — (Abbr. PT). A turbine stage in a gas turbine whose work output is used solely to drive the load with none being used by the compressor. In a 2-shaft gas turbine, the power turbine is fixed to a separate shaft from that of the GP turbine. It is normally -- but not required to be -- the last, or lowest pressure, turbine stage.

PR — Pressure Ratio. For a compressor or compressor stage, the ratio of outlet to inlet total pressure. For a turbine or turbine stage, the ratio of inlet to outlet total pressure.

PRIS — Particle Rejection Impact Separator. A device located between the primary and secondary zones of a rich-lean coal fired combustor which removes particulates from the gas stream.

PROFILE — The distribution of gas temperature within a single radial plane of a gas turbine combustor exit or other downstream annulus. The temperature profile represents the environment experienced by a turbine blade as it rotates through a temperature pattern thus averaging out circumferential variations. A "Profile Factor" can be defined using the Pattern Factor equation but confining the temperature data to a single radial plane.

PSR — Primary Surface Recuperator. Solar's proprietary design in which all heat exchange surfaces are "primary," i.e., transferring heat in their transverse direction. (A "secondary" surface, such as a fin, transfers heat in a lateral direction).

PT — See POWER TURBINE.

RECUPERATOR	A heat exchanger placed in the exhaust gas stream of a gas turbine in order to extract heat from the exhaust gases and return it to the cycle by heating the combustor inlet air. The term "recuperator" designates a static device as opposed to a "regenerator" which is a periodic device.
SHROUDED	A type of turbine blade design. A "shrouded" turbine features a short circumferential shroud segment attached to each blade tip. Together, these segments make up a full circular, rotating shroud. The outside surface of this shroud normally carries one or more circumferential seal elements. Conversely, a "non-shrouded" turbine is characterized by open blade tips rotating in close proximity to a stationary shroud.
SPOOL	The compression and expansion element of a gas producer, consisting of a compressor, a turbine and associated shafting. The turbine is designed so as to provide the amount of work required for the compression process plus any mechanical losses. A gas producer includes one or more spools and will be designated as 1-spool, 2-spool, etc.
SR	Stress Rupture. Stress rupture is the failure mechanism where gross rupture occurs due to time dependent deformation caused by steady stress at elevated temperatures. The mechanism at intermediate stages of deformation is called creep and is measured in terms of plastic strain. Stress rupture is usually associated with the Larson-Miller Parameter (LMP) which correlates the relationship between service life in hours and service temperature at a constant stress level. For a given material, Larson-Miller Parameter curves are developed which depict the LMP as a function of steady stress level.
STAGE WORK FACTOR	The ratio of work actually performed by a flow of cooling air within a turbine stage, to that possible if the flow were added to the hot gas stream.
STALL	A condition arising in one or more stages of an axial compressor in which the design pressure-velocity-rotational speed relationship is disrupted such that separation of the air flow from the blade contour occurs.
STANDBY	Use as a descriptor of a power generation station or unit that is only drawn upon when there is a demand. It currently is thought of as an emergency back-up unit in case the primary system fails, or when the primary unit cannot met the load demand. Sometimes called an "on-demand" system.
SURGE	The condition occurring when a compressor is operated below its minimum stable air flow rate for a given rotational speed. Surge is characterized by cyclic backflow of air in the flowpath accompanied by violent pressure fluctuations. During surge all stages of the compressor will be in a stall condition.
TBC	Thermal Barrier Coating. A thermally insulating ceramic coating (ZrO_2) applied to superalloy combustor and airfoil components. The insulative properties of the coating allow increased turbine inlet temperatures while maintaining acceptable metal substrate temperatures.

T&D	Transmission and Distribution. The system used to get the power (or fuel) from the point of origin to the consumer.
TRIT	Turbine Rotor Inlet Temperature. The average gas temperature entering the rotor annulus of the first turbine stage in a gas turbine. It is less than the average combustor exit temperature due to the mixing of spent cooling air flow from upstream sources, primarily the fist stage nozzle vanes.
TSSC	Two-Stage Slagging Combustor.
ZWEIFEL COEFFICIENT	A measure of turbine blade loading based on pitch/chord ratio and gas turning angle as independent variables.